NANO · MICRO small
www.small-journal.com

Gelatin Nanoparticles can Improve Pesticide Delivery Performance to Plants

*Sunho Park, Mahpara Safdar, Woochan Kim, Jaehwi Seol, Dream Kim, Kyeong-Hwan Lee, Hyoung Il Son, and Jangho Kim**

Nanomaterials associated with plant growth and crop cultivation revolutionize traditional concepts of agriculture. However, the poor reiterability of these materials in agricultural applications necessitates the development of environmentally-friendly approaches. To address this, biocompatible gelatin nanoparticles (GNPs) as nanofertilizers with a small size (≈150 nm) and a positively charged surface (≈30 mV) that serve as a versatile tool in agricultural practices is designed. GNPs load agrochemical agents to improve maintenance and delivery. The biocompatible nature and small size of GNPs ensure unrestricted nutrient absorption on root surfaces. Furthermore, when combined with pesticides, GNPs demonstrate remarkable enhancements in insecticidal (≈15%) and weed-killing effects (≈20%) while preserving the efficacy of the pesticide. That GNPs have great potential for use in sustainable agriculture, particularly in inducing plant growth, specifically plant root growth, without fertilization and in enhancing the functions of agrochemical agents is proposed. It is suggested conceptual applications of GNPs in real-world agricultural practices.

1. Introduction

Despite progress in agricultural prosperity, nearly one billion people worldwide still suffer from insufficient nutrient conditions, highlighting the need for an effective and productive agricultural system. The United Nations' 2030 agenda for sustainable development with 17 goals reaffirmed the importance of sustainable agriculture in achieving food security and improving nutrient availability.[1,2] Currently, the agriculture sector is confronted with various challenges including climate change, plant diseases, soil nutrient depletion, reduced crop yield, limited awareness of genetically modified crops, and workforce shortages, which threaten to destabilize agriculture sustainability.[3,4] Climate change exacerbates these issues, leading to more frequent and severe environmental stressors like salinity, drought, and temperature fluctuations, resulting in substantial annual declines in global crop production, yield, and quality.[5] To address these challenges, farmers have adopted the practice of excessive utilization of agrochemicals to manage these losses and enhance crop yields.[6] However, prolonged reliance on conventional fertilizers exacerbates environmental issues, including air pollution, soil degradation, water eutrophication, and groundwater contamination.[7,8] Moreover, chemical fertilizers exhibit low efficiency, as they are prone to volatilization and leaching, leading to environmental contamination and increased production costs, thereby hindering the attainment of agricultural sustainability.[9] Therefore, is an urgent need for novel strategies to optimize agrochemical usage, ensuring crop protection from environmental stressors, and meeting current and future food demands in a safe and sustainable manner.

Among the various alternatives for a productive agricultural system, nanotechnology is often suggested as an important tool in the impending agri-tech revolution.[10] Nanotechnology has shifted the direction of agricultural research toward identifying strategies that support sustainable agriculture incorporating food security and human health.[11–15] Especially, nanomaterial-based approaches serve as a bridge to fill the knowledge gap between ideal theoretical applications of nanotechnology and real-world solutions to existing problems in agricultural practice.[16] Nanomaterials (NMs) are considered as an ideal platform for advancing the agri-nanotech revolution due to their ultra-small size (< 100 nm), enabling them to traverse biological barriers and penetrate plant tissues through foliar or root application, thus offering innovative and efficient pathways for delivering nutrients and pesticides.[17,18] The optimal applications of NMs in

S. Park, M. Safdar, W. Kim, J. Seol, D. Kim, K.-H. Lee, H. I. Son, J. Kim
Department of Convergence Biosystems Engineering
Chonnam National University
Gwangju 61186, Republic of Korea
E-mail: rain2000@jnu.ac.kr

S. Park, M. Safdar, W. Kim, J. Seol, D. Kim, K.-H. Lee, H. I. Son, J. Kim
Department of Rural and Biosystems Engineering
Chonnam National University
Gwangju 61186, Republic of Korea

S. Park, M. Safdar, W. Kim, J. Seol, D. Kim, K.-H. Lee, H. I. Son, J. Kim
Interdisciplinary Program in IT-Bio Convergence System
Chonnam National University
Gwangju 61186, Republic of Korea

S. Park
Department of Bio-Industrial Machinery Engineering
Pusan National University
Miryang 50463, Republic of Korea

The ORCID identification number(s) for the author(s) of this article can be found under https://doi.org/10.1002/smll.202402899

DOI: 10.1002/smll.202402899

agriculture include nanofertilizers to enhance growth and crop productivity, disease suppression, and nanosensors for monitoring soil quality and plant health.[19,20] In agriculture, NMs offer a means to deliver herbicides, fertilizers, and pesticides more effectively, with a larger specific surface area enabling "on-demand" release to combat pathogens, pests, and diseases, while also meeting nutritional needs, ultimately promoting improved crop growth, yield, and quality.[21,22] For instance, Liu et al. demonstrated that surface charge-modified carbon-based nanomaterials (i.e., carbon nanotubes; CNTs) with macromolecules including single-stranded DNA and a fluorescent dye macromolecules could penetrate the hard plant cell wall and membrane, showing potential as a carrier to deliver materials to a specific site in plant cells.[23] This discovery helped to resolve the challenge of high-efficiency delivery of molecules and vectors into living plant cells, enabling new developments of nanomaterial-based plant biology such as gene delivery, sensing, and imaging.[19,24–29] NMs can also be used as innovative tools in agriculture, including food production and the floricultural industry.[30–33] However, some problems related with these NMs, including accumulation, concentration-dependent cytotoxicity and non-degradability.[34,35] Additionally, their application has generally been performed under controlled laboratory conditions; thus, a pragmatic solution is needed for real-world application in an agricultural setting.[36]

To enhance the utilization of nanoparticles, we designed biocompatible gelatin-derived versatile nanoparticles (GNPs) characterized by a uniform spherical structure. In a prior study, gelatin-based fertilizer was introduced. Sathisaran and Balasubramanian reported that chitosan/gelatin/alginate beads can regulate the release of urea.[37] Juan-Martínez et al., fabricated gelatin particles for loading calcium.[38] While the potential use of these materials in agriculture has been noted, our objective was to delve into their applicability in more detail. We present the initial empirical evidence and the first real-world confirmation that raw GNPs can induce plant root growth, and agrochemical-blended GNPs can effectively combat weeds and insects, demonstrating their potential as a versatile material with applications in agricultural fields.

2. Results

2.1. Design and Characteristics of the Versatile GNPs

We propose a solution for reducing the intensive use of agrochemicals, like pesticides, and improving their functions using biocompatible nanomaterials (GNPs) in agricultural fields. The current challenges facing agriculture are the reduction of the intensive use of agrochemicals, like pesticides, and improvement in their functions can help to reduce the workload of local farmers and environmental pollution. One solution is the gradual release of agrochemicals, which can be achieved using GNPs, which is one of nitrogen-rich fertilizer.[39,40] These versatile GNPs have desirable properties that are summarized in **Figure** 1a. GNPs have been used for drug loading and can achieve gradual release of agrochemicals. It is ideal for promoting the delivery and maintenance of a pesticide or herbicide on the leaf surface.[41] To investigate these abilities of GNPs, we confirmed plant growth based on their biocompatibility using *A. thaliana* and grass models, and further explored the insecticidal and weed-killing effects of GNPs loaded with an insecticide and herbicide.

As shown in Figure 1b, we fabricated GNPs with high uniformity and stability using the two-step desolvation method through increasing the compression between molecules and decreasing the volume as the temperature is reduced.[42] It was reported that autoclave sterilization of gelatin nanoparticles results in the partial release of gelatin molecules and slight nanoparticle growth, but higher cross-linking degrees and milder autoclaving conditions make nanoparticles less sensitive to thermal degradation.[43]

The spherical structure of GNPs with non-aggregation and uniformity was confirmed by scanning electron microscopy (SEM), showing an average diameter of ≈143.6 nm (Figure 1c,d). Furthermore, GNPs in the pesticide solution exhibited average diameters of 248 nm, 4.300, and 90.6 µm, suggesting the swelling and aggregation of GNPs under these solution conditions (Table S1, Supporting Information). GNPs showed an identical peak to that of raw gelatin in Fourier transform-infrared (FT-IR) spectroscopy, indicating an amide-A peak arising from N-H stretching of the cross-linking degree at 3466 cm^{-1}, an amide I peak arising from C = O stretching at 1630 cm^{-1}, and amide II peaks of N-H deformation and C-N stretching at 1565 cm^{-1} (Figure 1e).[44] The zeta potential of GNPs suspended in pure deionized water was ≈ +29.95 mV with mobility of 2.336 µmcm Vs^{-1}, indicating the positively charged surface property of GNPs (Figure 1f). The leaf surface generally has a negative charge owing to the epicuticular wax crystals and the fatty acids that prevent water evaporation and defend against pathogen infection; thus, use of GNPs with agrochemicals could aid in the delivery and attachment to the leaf surface.[45,46]

We further investigated the drug release from GNPs using trypan blue as a model drug with different concentrations (0.015, 0.03, and 0.06 g mL^{-1}) (Figure 1g). The drug was rapidly released from GNPs with an initial burst in the first 3 days because of adsorption onto the external surface of GNPs and the weak mechanical properties of gelatin. The release rate of GNPs with 0.06 g mL^{-1} trypan blue was the highest due to the diffusion phenomenon related to the model drug release from solid materials (Figure S1, Supporting Information). As shown in data, the initial burst as well as the release curves were slightly different depending on the concentration, but the trend was similar for all three drugs concentrations. At different temperatures (4, 18, and 36 °C), the release rate shows a similar trend after an initial burst in the first 3 days (Figure S1b, Supporting Information). In the next step, we performed a time-dependent surface chemical analysis of pesticide-loaded GNPs using FT-IR analysis, indicating a broad band between 2858 and 3010 cm^{-1} corresponded to the C–H stretching vibration, some relatively weaker bands located ≈1500 and 1850 cm^{-1} resulted from aromatic ring vibrations overlapping with C═N vibrations, a strong peak peak at ≈925 cm^{-1} resulted from C–N stretching vibrations, and a band occurring at ≈750 cm^{-1} was assigned to C–S vibrations (Figure 1h).[47] The results revealed that over time, the characteristic peaks associated with the pesticide in the pesticide-loaded GNPs started to decrease, indicating that the pesticide was gradually being released from the GNPs. This finding suggests that the GNPs have the potential to function as carriers for controlled release of pesticides, which could have

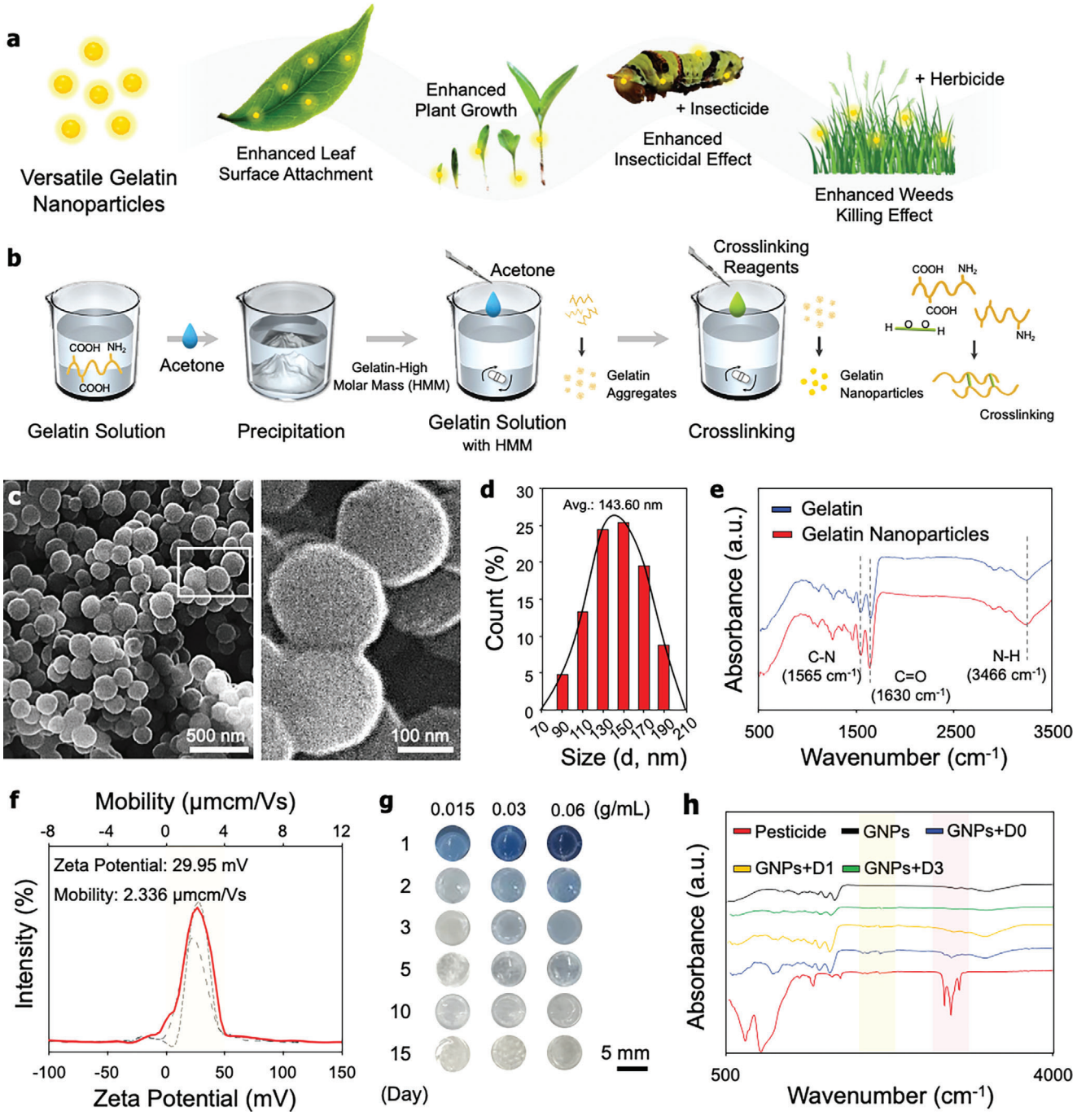

Figure 1. Biocompatible gelatin nanoparticles (GNPs) as versatile tools for advanced applications in agriculture. a) Schematic of the ideal applications of GNPs. The proposed GNPs might be used to enhance the leaf attachment, plant growth, then insecticidal effect and killing effect after the combination with agrochemical materials. b) Schematic of the fabrication process of GNPs using two desolvation method. c) Scanning electron microscope images of the fabricated GNPs with high magnification. d) Size distribution histogram of nanoparticles. e) Fourier-transform infrared (FT-IR) spectroscopy spectra of GNPs. f) Zeta potential and mobility of GNPs. Red line shows the average of Zeta potential and mobility of GNPs. g) in vitro release test using model drug (i.e., trypan blue). Photograph of the released trypan blue solution from GNPs for 15 days. Drug release profile from GNPs of 0.03 g with a 0.015, 0.03, or 0.06 g mL^{-1} solution of a trypan blue for 15 days. h) FT-IR spectroscopy spectra of GNPs and pesticide-loaded GNPs before and after washing. The washing process involved three cycles, conducted once a day. Error bars represent the standard deviation about the means (n = 3 for each group).

implications for enhancing the efficacy and safety of pesticide applications.

We have investigated the fertilizer loading efficiency on GNPs with varied urea-to-gelatin ratios in composition, as depicted in Figure S2a (Supporting Information). The urea uploading on GNPs was improved by gradually increasing the GNPs concentration at 1:2 ratio. However, when the urea-to-gelatin ratio changed from 1:1 to 2:1, there was a decrease in urea loading efficiency. In urea-to-gelatin ratios, the greatest urea uploading was observed at 1:2 (52.46%), while the lowest urea uploading efficiency was obtained at 2:1 (38.16%) on day-5. We believe that the declining pattern in urea uploading efficiency is caused by the reduced gelatin-to-urea ratio. Moreover, it is well-established that an excess of urea can hinder the formation of hydrogen bonds (H-H), thereby reducing the risk of further urea entrapment within the loose and poorly constructed inner structure of GNPs.[48] To overcome this obstacle, more GNPs has been added to find improvement in uploading and trapping efficiency.

Furthermore, we also investigated the release dynamics of urea from GNPs containing various concentrations (0.015, 0.03, and 0.06 g mL^{-1}) at room temperature, as depicted in Figure S2b (Supporting Information). Following day-1, a slow and gradual release of urea was observed from GNPs across all compositions, exhibiting a concentration-dependent pattern. The release percentage of urea from GNPs remained slow and minimal at 0.015 g mL^{-1} concentration, whereas at higher concentrations (0.03 and 0.06 g mL^{-1}), a more rapid release was initiated. The urea that is either poorly confined or radily present on the surface of GNPs is released steadily initially at slow rate and the urea that is fully trapped in the cross-linked network of the GNPs is released over time through a diffusion process, as evidenced by the later release after day 1, which is comparatively slower. These findings underscore the potential of GNPs to serve as carriers and make significant contributions to the development of affordable and more effective GNPs-based slow-release fertilizers, thereby promoting agricultural sustainability.

2.2. Effects of the Versatile GNPs on Plant Growth

GNPs synthesized from a bioresource, specifically gelatin derived from porcine skin and cartilage, have shown potential as a fertilizer for controlling plant properties, including germination and growth.[49,50] To test whether our GNPs can regulate plant growth, we conducted experiments on *A. thaliana* as a plant model (**Figure 2**a). After reaching the seedling stage, *A. thaliana* seedlings were transplanted onto agar plates with and without GNPs. Root and leaf growth were visibly promoted by day 10 (Figure 2b,c). To confirm the specific effects of GNPs on plant growth, we quantified the root length, leaf area, fresh weight, and leaf number on days 3 and 10 (Figure 2d–g). We found no significant differences in root length and leaf area at day 3, whereas the root length and leaf area of GNP-treated *A. thaliana* increased significantly compared to untreated plants. GNP-treated *A. thaliana* also weighed more and had a higher leaf number than untreated plants. Microscopy and toluidine blue staining showed that the cells in GNP-treated *A. thaliana* had a plumb structure, and the aspect ratio (horizontal and vertical length) showed a larger perimeter and area of the root cells (Figure 2h). Additionally, the root cell shape index of GNP-treated *A. thaliana* indicated a spherical cell morphology (index close to 1), similar to that of untreated *A. thaliana*. These findings suggest that GNPs can interact with the root and cells, affecting plant growth without cytotoxicity. As shown in Figure 2i, there were no significant differences in stoma perimeter, but the density of the stoma in GNP-treated *A. thaliana* was higher than that in untreated *A. thaliana*. A larger stoma size indicates reduced stomatal density, which could reduce water transpiration as a suitable response to stress for better water use efficiency.[51,52] To confirm the interaction of GNPs with plant roots, the surface structure was confirmed by SEM (Figure 2j). The root surface of GNP-treated *A. thaliana* was entirely covered by GNPs, which had a collapsed spherical structure at the nanoscale, whereas the root surfaces of untreated *A. thaliana* had a smooth surface. During growth, the root interacted with GNPs on the agar plate, which might have been adsorbed into the root surfaces. We also detected the expression of root growth-related genes, but only a slight difference was observed, indicating that GNPs had positive effects on root growth (Figure 2k).

We also investigated the expression of root growth-related genes, but only a slight difference was observed compared to control, indicating that GNPs had positive effects on root growth (**Figure 3**k). Notably, transcription factors such as *PLETHORA1 (PLT1)* and *PLT2* play pivotal roles in maintaining the primary root meristem, activated in the basal embryo region, ultimately leading to the development of the hypocotyl, root, and root stem cell.[53] Additionally, *PLT1* and *PLT2* expressions are closely linked to a maximal transcriptional response to the plant hormone auxin in the root tip. This maximal response has been demonstrated to possess significant organizing activity, aligns with characteristics often associated with sources of instructive gradient.[54] Auxin, a pivotal plant hormone, is essential for regulating root development, with optimal concentrations facilitating elongation and excessive accumulation hindering it. The precise control of the auxin concentration gradient in the root is achieved through the regulation of auxin biosynthesis and transport.[55] The PIN family genes stand out as the most extensively studied efflux auxin transporters. Among the eight PINs identified in *A. thaliana*, namely PIN1, PIN2, PIN3, PIN4, and PIN7, they collectively govern the distribution of auxin in roots and are key contributors to the intricate process of root elongation.[56,57] According to the Starch–Statolith hypothesis, the sedimentation of amyloplasts in gravity-sensing cells, such as root columella cells, initiates biochemical signals, including auxin. Upon gravity stimulation (reorientation) of primary roots, the subcellular localization of auxin transporters, particularly PIN-FORMED (PIN) proteins like PIN3 and PIN7, undergoes repolarization. This results in a redirection of auxin flux towards the lower side of the root, subsequently causing differential cell elongation and bending at the root tip.[58] *CYTOKININ RESPONSE FACTOR2 (CRF2)* and *CRF3*, encoding APETALA2 transcription factors, play a crucial role in regulating the initiation of lateral roots in *Arabidopsis*. These roots serve as a primary determinant of the plant's root system architecture, and the developmental flexibility in lateral root formation is vital for plant survival amidst changing environmental conditions.[59] The *AUX1/LAX* gene family, consisting of *AUX1*, *LAX1*, *LAX2*, and *LAX3*, with 75%–80% protein-level similarity, functions as major auxin influx carriers. Among them, *AUX1* has been extensively studied and demonstrated to

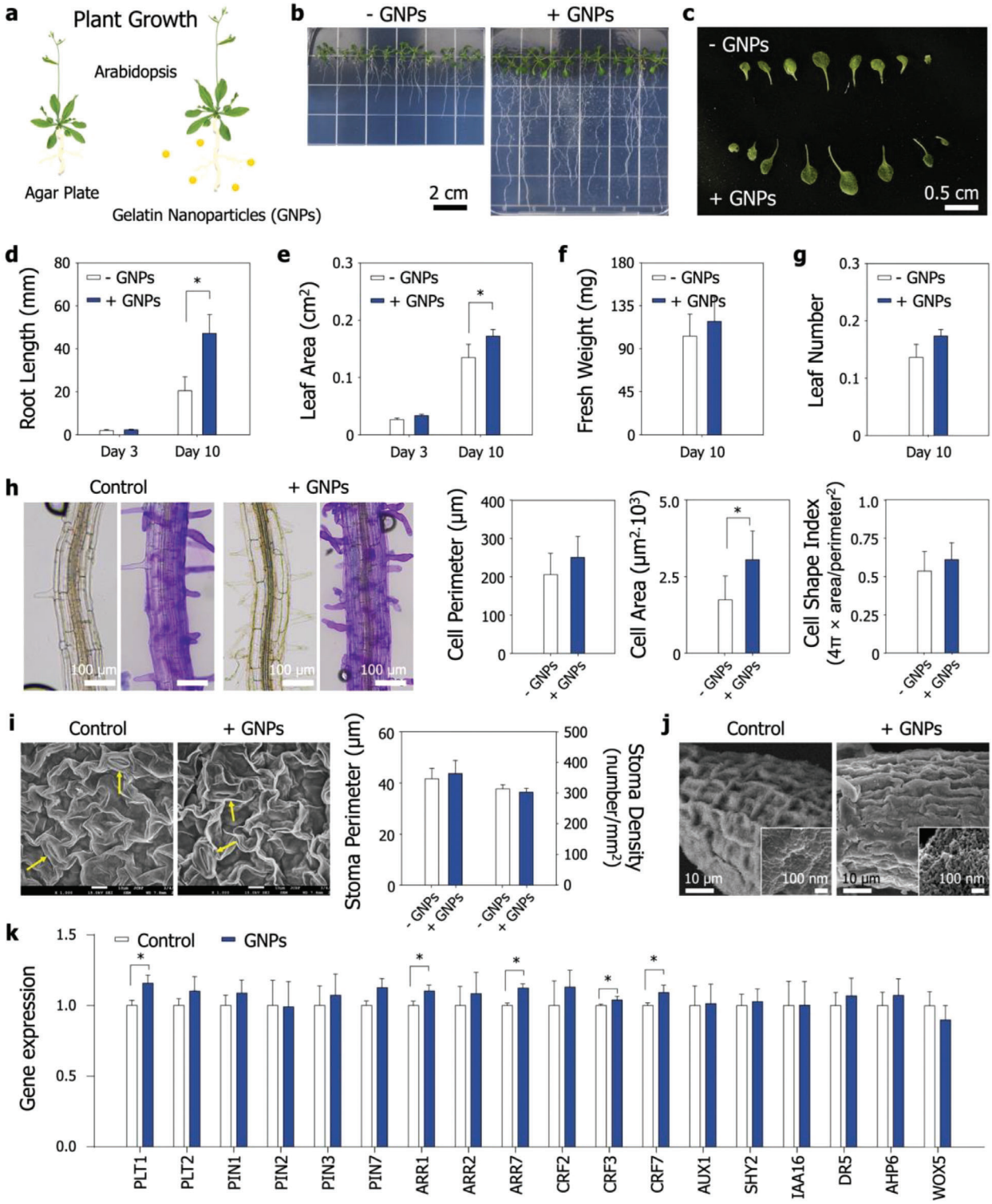

Figure 2. Enhanced plant root growth with or without biocompatible gelatin nanoparticles (GNPs) using *A. thaliana*. a) Schematic of the plant root growth on agar plates with and without GNPs. b and c) Representative photograph of *A. thaliana* on an agar plate with and without GNPs after 2 weeks. d–g) Quantification of root length, leaf area fresh weight, and leaf number after 3 and 10 days. h) Representative root and toluidine-stained root images, and quantification of cell perimeter, area, and cell shape index of *A. thaliana* on agar plates with and without GNPs. Data were analyzed by Student's *t-test* ($^*P < 0.05$). i) Representative scanning electron microscope (SEM) images, and quantification of stoma perimeter and stoma density on the leaf surfaces of *A. thaliana* with and without GNPs at 10 days. j) Representative SEM images of root surfaces of *A. thaliana* with and without GNPs at 10 days. k) Plant root growth-related gene expression of *A. thaliana* with and without GNPs at 10 days (a.u.). Error bars represent the standard deviation of means (n = 5 per group). Data were analyzed by Student's *t-test* ($^*P < 0.05$).

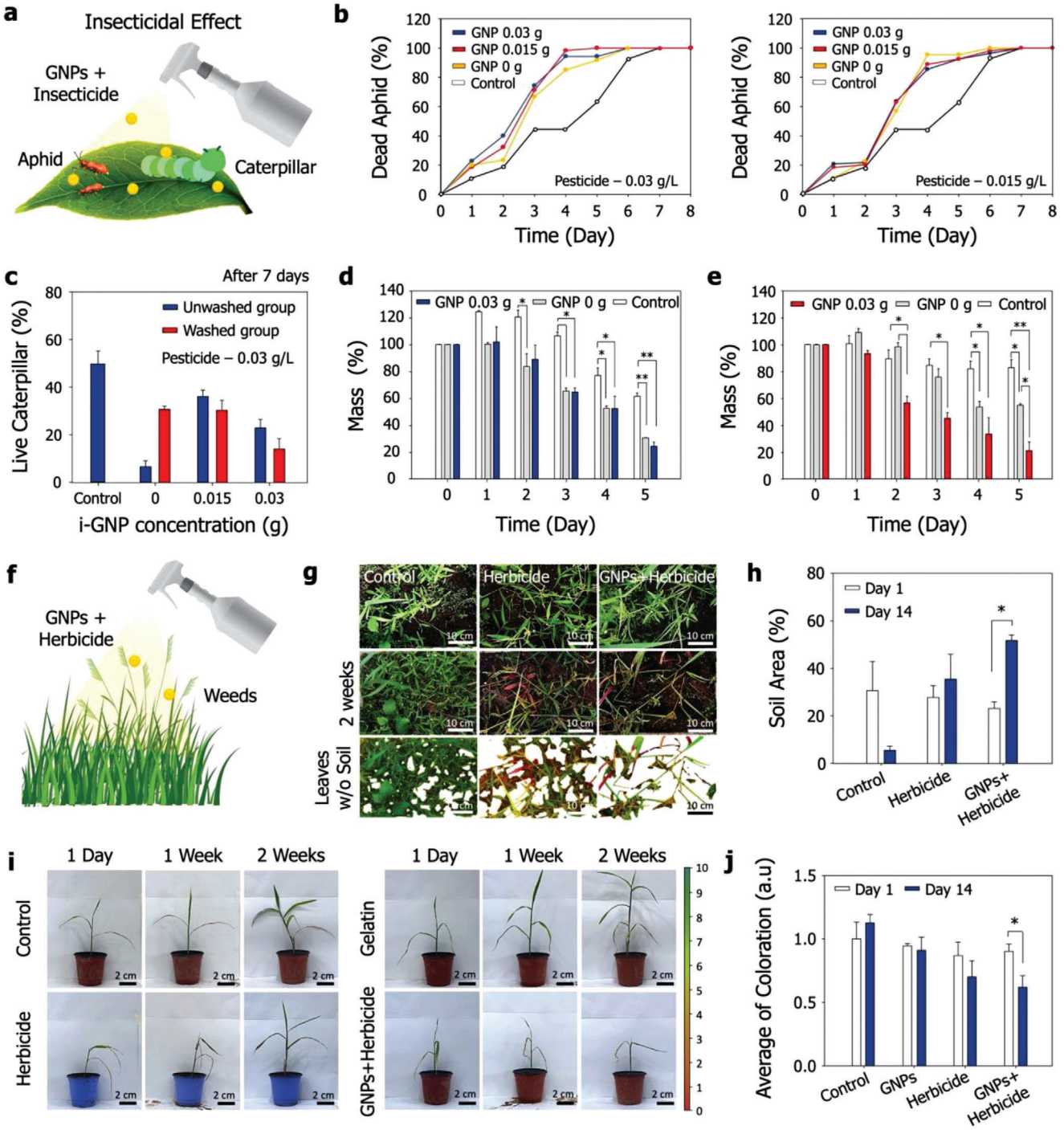

Figure 3. Enhanced insecticidal and weed-killing effects of biocompatible gelatin nanoparticles (GNPs) using aphids, larvae, and weeds. a) Schematic of the insecticidal effects of GNPs with insecticide on aphids and larvae. b) Concentration-dependent insecticidal effects of GNPs on aphids. GNPs with 0.03 g L^{-1} (left) and 0.015 g L^{-1} (right) insecticide. Data were analyzed by Student's *t* test (*$P < 0.05$). c) Concentration-dependent insecticidal effects of GNPs on larvae before and after washing. GNPs with 0.03 g L^{-1} insecticides. Data were analyzed by Student's *t* test (*$P < 0.05$). d and e) Quantification of mass change of larvae before (left) and after (right) washing. Data were anlayzed using one-way ANOVA (*$P < 0.05$,**$P < 0.01$). f) Schematic of the weed-killing effects of GNPs with herbicide on weeds. g) Representative photograph of weeds before and after treatment with herbicide and GNPs with herbicide. h) Quantification of the soil area at day 1 and day 14 before and after treatment with herbicide with or without GNPs. Data were analyzed by Student's *t* test (*$P < 0.05$). i) Representative photograph of a single weed after treatment with GNPs, herbicide, and GNPs with herbicide. j) Quantification of the coloration of weed leaves at day 1 and day 14. Data were analyzed by Student's *t* test (*$P < 0.05$). Error bars represent the standard deviation of means (n = 5 per group).

govern root gravitropism and lateral root development.[60] Furthermore, the *SHY2* gene encodes *IAA3*, a recognized member of the *Aux/IAA* family of auxin-induced genes. *SHY2/IAA3* influences auxin-dependent processes in roots, including root growth, lateral root formation, and gravitropism, highlighting its role in regulating multiple auxin responses.[61] Additionally, key transcription factors (TFs) *WUSCHEL-RELATED HOMEOBOX 5 (WOX5)* and *PLETHORAs (PLTs)* are actively expressed within the *Arabidopsis* roots stem cell niche (SCN). This niche is indispensable for the growth and development of all root cell types, playing a dual role in maintaining the quiescent center (QC) and regulating the fate of distal columella stem cells (CSCs).[62] These data indicate that GNPs are essential for root development and may have a broad role in different developmental processes by tightly regulating different family genes signaling.

Furthermore, we checked the antibacterial effects of GNPs because microorganisms are important factors in agriculture.[63,64] GNPs did not exhibit antibacterial effects and had no bacterial zone of inhibition (Figure S3a, Supporting Information). These findings demonstrated that raw GNPs would not be cytotoxic to plants or microorganisms in agricultural fields and would not inhibit plant or microorganism activities.

To validate the potential of GNPs as nanofertilizers in promoting plant growth, we conducted experiments using *A. thaliana* as a plant model. Upon reaching the seedling stage, *A. thaliana* seedlings were transplanted onto agar plates divided into two groups: with GNPs and without N (+ GNPs − N), and without GNPs (− GNPs + N) as a control. By day 10, noticeable enhancements in root and leaf growth were observed (Figure S4a,b, Supporting Information). To confirm the specific effects of GNPs on plant growth, we quantified various parameters including seedling fresh weight, root length, leaf number, leaf area and lateral root number on days 3 and 10 (Figure S4c–g, Supporting Information). Our results indicated that all phenotypic aspects of *A. thaliana* cultured in GNPs-treated media without nitrogen were significantly increased compared to untreated plants grown in media containing nitrogen. Furthermore, we conducted microscopic analysis of root cell parameters, area, and cell shape on day 10, revealing a significant increase in both cell parameter and area in the GNPs-treated samples without nitrogen compared to those grown in media containing nitrogen (control growth) (Figure S4h, Supporting Information). These findings strongly suggest that GNPs possess the ability to promote plant growth by functioning as nano-fertilizers, thus contributing to agricultural sustainability.

In order to assess the potential of Gelatin NPs (GNPs) in real agricultural contexts, distinct from the *A. thaliana* model plant, we conducted experiments utilizing *Camelina sativa* as our crop model. Following germination, equally germinated seedlings were transplanted into agar magenta boxes, both with and without the inclusion of GNPs. By day 10, notable enhancements in root, stem, and leaf growth were observed in the Gelatin NPs-treated plants (Figure S5a–c, Supporting Information). To validate the specific effects of GNPs on crop growth, we meticulously quantified various parameters including fresh seedling weight, stem and root length, leaf number, and leaf area at both day 3 and day 10 post-transplantation (Figure S5d–h, Supporting Information). Our findings indicated that *Camelina sativa* treated with GNPs exhibited higher weight and leaf count compared to untreated crops. Moreover, the stem and root lengths of GNPs-treated crops showed significant increases compared to the untreated group. These results strongly suggest that GNPs can positively influence crop growth by interacting with crop roots and cells, thereby promoting growth without inducing any cytotoxic effects.

2.3. Killing Effects of Insecticide and Herbicide-Loaded GNPs on Insects and Weeds

GNPs can load and release materials, while improving attachment and maintenance on the leaf surface (Figure 1 and Figure S3b,c, Supporting Information). To confirm these effects, the pesticide was diluted with water (0.015 and 0.03 g L^{-1} – recommended concentration), and the same or a lower amount of GNPs (0.015 and 0.03 g) was added to the diluted pesticide solution (Figure 3a). The absorption and loading of insecticide onto GNPs are facilitated by electrostatic interactions between the pesticide (i.e., insecticide and herbicide) and the carbonyl groups (C═O) of the amide on the GNPs.[38] The insecticidal effect of insecticide-loaded GNPs (i-GNPs) was then confirmed in vivo using aphids and caterpillars (*Pieris rapae*; *P. rapae*) in the controlled condition (sealed dishes without external effects). The number of dead aphids increased over time after treatment with both the insecticide and i-GNPs; however, i-GNPs showed an improved and faster insecticidal effect compared with insecticide treatment alone (Figure 3b). In the early stage (≈3 days), the ratio of dead aphids was higher with i-GNPs of 0.03 g but increased with i-GNPs of 0.015 g at the later stage (days 4–7) without external effects. We then tested a reduced volume of the insecticide to determine whether the use of GNP reduces the pesticide amount required to kill insects effectively. The dead aphid rate tended to slow down but was higher with the insecticide-treated samples, indicating that an optimal volume is required for loading GNPs. However, the killing effects of i-GNPs were still higher than those of the insecticide in the early stage. For the caterpillar test, more than half of the caterpillars of the control group survived after 7 days. Pesticides are typically washed away by water and rain; thus, we compared the effects of i-GNPs and insecticide with/without washing (Figure 3c).[65] The unwashed group showed high insecticidal effects, whereas the effect of the washed group was substantially reduced, demonstrating that the pesticide was readily washed off the leaf. In contrast, the numbers of live caterpillars treated with i-GNPs decreased even after washing, confirming that the retained GNPs still contained the insecticide to cause the damage to the caterpillar. The number of live caterpillars was the highest in the control, followed by the 0.015 g, 0.03 g i-GNPs, and pesticide without washing groups. As shown in Figure 3d,e, in the early stages, the mass of the caterpillars in the control group increased with insect growth, whereas the mass decreased after pesticide treatment, and significantly decreased further after treatment with i-GNPs both before and after washing. In contrast, mass reduction slowed down over time by treatment with only pesticide, showing a diminished insecticidal effect. After four days, discharge was observed from the damaged larva, and it subsequently turned black, indicating its death (Figure S6, Supporting Information). Thus, GNPs might

improve the attachment and maintenance of agrochemical materials.

Crop growth is often disturbed by over 200 species of weeds, with ≈30 species being particularly responsible for serious crop yield losses.[66] To address this issue, herbicides are widely used to damage weed. However, the excessive use of herbicides is associated with several problems, such as the development of weed resistance, which leads to a reduced killing effect.[67–69] To overcome this challenge, we investigated the killing effects of herbicide-loaded GNPs (h-GNPs) on weeds (Figure 3f). After two weeks, we observed that the ground was completely overgrown with weeds in untreated soil, indicating rapid adaptation (Figure 3g). However, the areas sprayed with herbicide and h-GNPs had a reduced weed density, showing increased soil area (Figure 3h). Because weeds have high viability and adaptability, we also evaluated the lasting killing power of one-time herbicide and h-GNPs treatment in single weed (Figure 3i,j). After the first week, we observed that the weeds, and one-time treatment of herbicides and h-GNPs resulted in weak weed growth. After two weeks, we found that the weeds in the herbicide-treated group became healthy with high viability, whereas those of the h-GNPs-treated group lost their viability.

The widespread use of urea as a nitrogen fertilizer presents a challenge due to its rapid volatilization into ammonia, leading to significant nitrogen loss from the soil.[70] To address this issue and enhance agricultural productivity while minimizing environmental impact, there has been a growing interest in developing efficient and eco-friendly fertilizers. In recent years, polymer-based controlled-release formulations have emerged as promising alternatives to traditional chemical fertilizers. These formulations not only help maintain soil fertility but also mitigate soil pollution and plant toxicity in agricultural areas.[37] To investigate the concentration-dependent effects of urea-loaded Gelatin NPs (U-GNPs), we seeded *Camelina sativa* in magenta boxes and compared growth phenotypic aspects among various groups, including Control, urea (0.015 and 0.03 g/150 ml), GNPs (0.015 and 0.03 g/150 ml), and U-GNPs (0.015 and 0.03 g/150 ml) at days 3 and 14 (**Figure** 4a). The loading efficiency and kinetic releases of urea onto the GNPs are facilitated by hydrogen bonds forming between GNPs and urea, leading to improved urea entrapment within GNPs in a concentration-dependent manner.[71] To confirm the specific effects of fertilizers loaded with and without GNPs on crop growth, we quantified seedling fresh weight, stem length, root length, leaf number, and leaf area at days 3 and 14 (Figure 4b–f). Our findings revealed that U-GNPs significantly promoted seedling weight, stem length, and root length compared to other groups. Moreover, the leaf number and area of *Camelina sativa* were significantly enhanced by U-GNPs compared to control groups. Additionally, we investigated the chlorophyll content of *Camelina sativa* fresh leaves on day 14, as chlorophyll content serves as a robust indicator of photosynthesis pathways.[72] Among all groups, chlorophyll buildup in the urea group (0.03 g/150 ml) increased up to 2.078 mg g^{-1}, whereas in GNPs-containing groups, chlorophyll content slightly reduced compared to the control (Figure 4g). These findings suggest that direct application of urea on *Camelina sativa* seedlings result in rapid nitrogen absorption, while the inclusion of GNPs enhances the encapsulation and entrapment of urea by forming hydrogen bonds, thereby promoting the steady release of fertilizer in a concentration-dependent manner.

The resistance of fertilizers to rain is another key factor that should be considered to improve fertilizer retention. As shown in Figure S7a (Supporting Information), when *Camelina sativa* leaves were treated with urea mixed with water, only ≈7.64% of urea was retained on the leaves after rain washing. However, when GNPs are incorporated with different concentrations, i.e., 0.015, 0.03 and 0.06, the retention rate of urea can reach 19.98%, 41.19%, and 62.16%. This shows that GNPs have advantages in improving the rain-fastness of fertilizers and can effectively reduce the migration of fertilizers on real crop leaves, which is beneficial to improve the utilization efficiency of fertilizers and reduce fertilizers loss.

2.4. Conceptual Applications of the Versatile GNPs in Real Agricultural Fields

To further evaluate the potential of GNPs in real agricultural fields, we established a field model and closely observed the effects on plant growth and pesticide activity. Commercial grass was seeded in commercial soil with and without GNPs. After 14 days, the grass sprouted, and the number of the grass plants was higher in GNP-treated group (**Figure** 5a,b). The growth rate of GNPs-treated grass was faster than that of the untreated group over 30 days. The number of germinated grass and the leaf area increased over time (Figure 5c). The average leaf area at day 30 was higher in the GNPs-treated group (Figure 5d). Notably, the difference in grass growth between raw grass and GNP-treated grass presented a time-dependent trend, with a high range at 2–3 weeks, which was inferred from the gradual effects of GNPs in the soil. Finally, we tested whether GNPs with herbicide affect weed killing in a real agriculture field using a commercial pest control machine. To our knowledge, this is the first confirmation of the effects of nanomaterials, including nanoparticles, in a real agriculture setting using a large volume (3 g GNPs, 100 mL herbicide, 100 L water). The herbicide solution with or without GNPs was sprayed onto the weeds at the real farm, and we confirmed that the spraying was not prevented by the addition of GNPs, indicating that the spraying nozzle system was not inhibited (Figure 5e,f). After 2 months, the weed-removed space after treatment of h-GNPs was larger than that after treatment of herbicide alone (Figure 5g).

Furthermore, we have focused our investigation on the potential of Gelatin NPs (GNPs) in agricultural applications, particularly in comparison to other established nanomaterials for fertilizer delivery. To address this, we conducted experiments using *Camelina sativa* grown in magenta boxes, wherein urea (U) served as the control, and urea-nanomaterial formulations were closely observed for their effects on growth at days 3 and 14 (Figure S8a–c, Supporting Information). Our study compared the efficacy of GNPs with two prominent nanomaterials, Graphene oxide (GO) and PCN-224, for fertilizer delivery in *Camelina sativa*. We assessed various growth parameters including fresh seedling weight, root and stem length, leaf number, and leaf area at both time points (Figure S8d–h, Supporting Information). The results revealed a notable increase in fresh seedling weight by day 14. Importantly, the crop treated with U-GNPs exhibited significantly

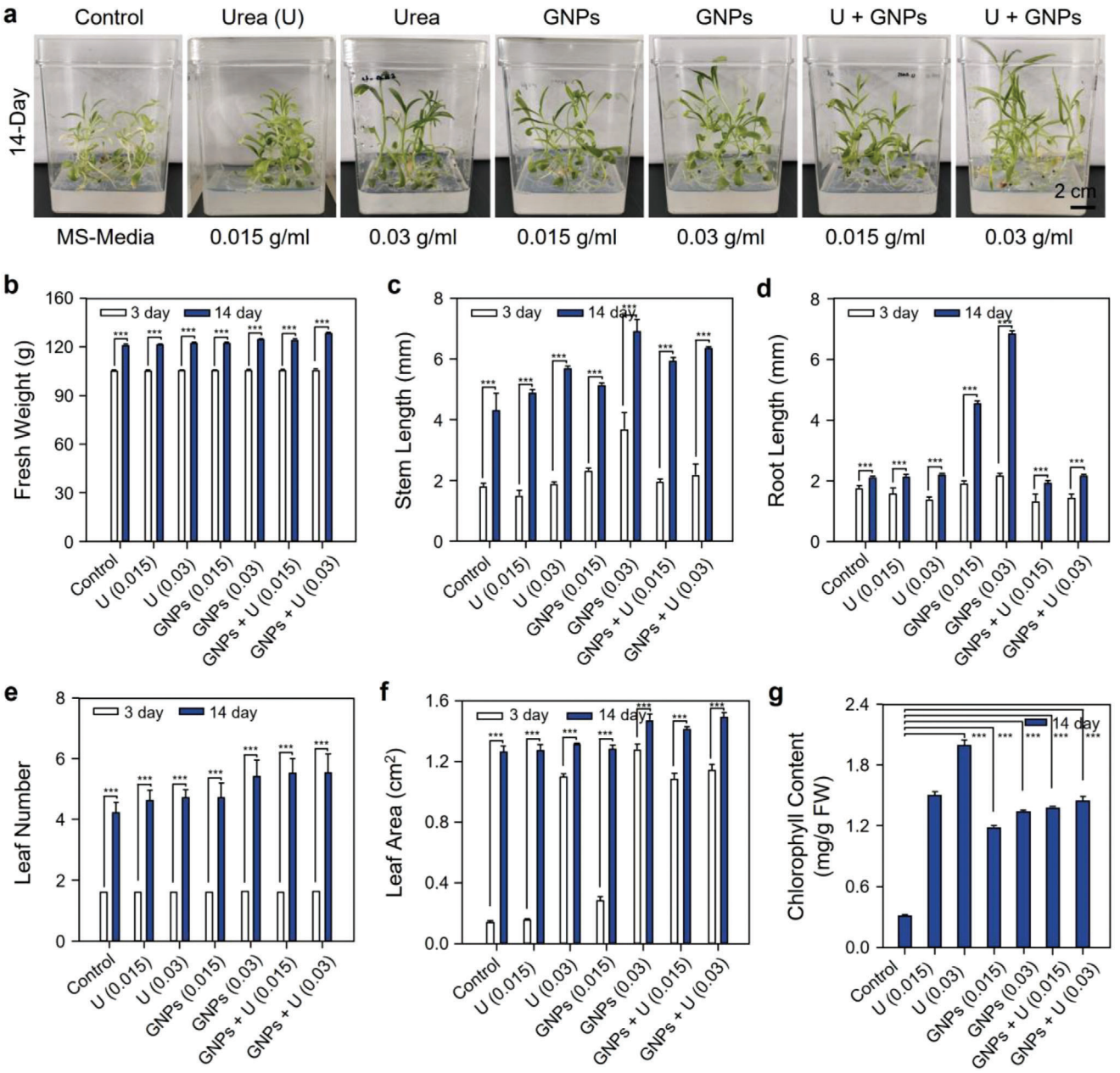

Figure 4. Potential application of biocompatible gelatin nanoparticles (GNPs) for fertilizer (urea) delivery effects on *Camelina sativa*. a) Representative photograph of *Camelina sativa* on agar-based magenta boxes with and without urea and GNPs after 14-days. b–f) Quantification of fresh weight, stem length, root length, leaf number and leaf area after 3 and 14 days. g) Quantification of chlorophyll content of fresh leaves on day 14. Error bars represent the standard deviation of means (n = 3 per group). Data were analyzed by Student's t test (*$P < 0.05$, **$P < 0.01$, ***$P < 0.001$).

enhanced root and stem length, leaf number, and leaf area compared to those treated with U-GO, U-PCN, and the control group. Additionally, we investigated the chlorophyll content in fresh leaves of all groups on day 14. Interestingly, we found that the chlorophyll content was higher in the control group compared to the U-GNPs, U-GO, and U-PCN groups (Figure S8i, Supporting Information). This suggests that among the various nanomaterials, GNPs are designed to deliver plant nutrients in a controlled manner, ensuring that the nutrients are gradually released over an extended period, thus providing a steady supply of essential elements to the plants facilitate a slower and more controlled release and delivery of fertilizers in crops. They can also improve fertilizer use efficiency, leading to higher crop yields and reducing the overall cost of fertilizer application.

To confirm the possible effects of GNPs on spraying form, we used LiDAR-based detection of droplets from the spray nozzle (**Figure 6a**). The detection data revealed that the spraying form with GNPs have a more spreader space than the spraying form without GNPs after the spraying from the nozzle. Sprayed droplets with GNPs were further apart than those without GNPs

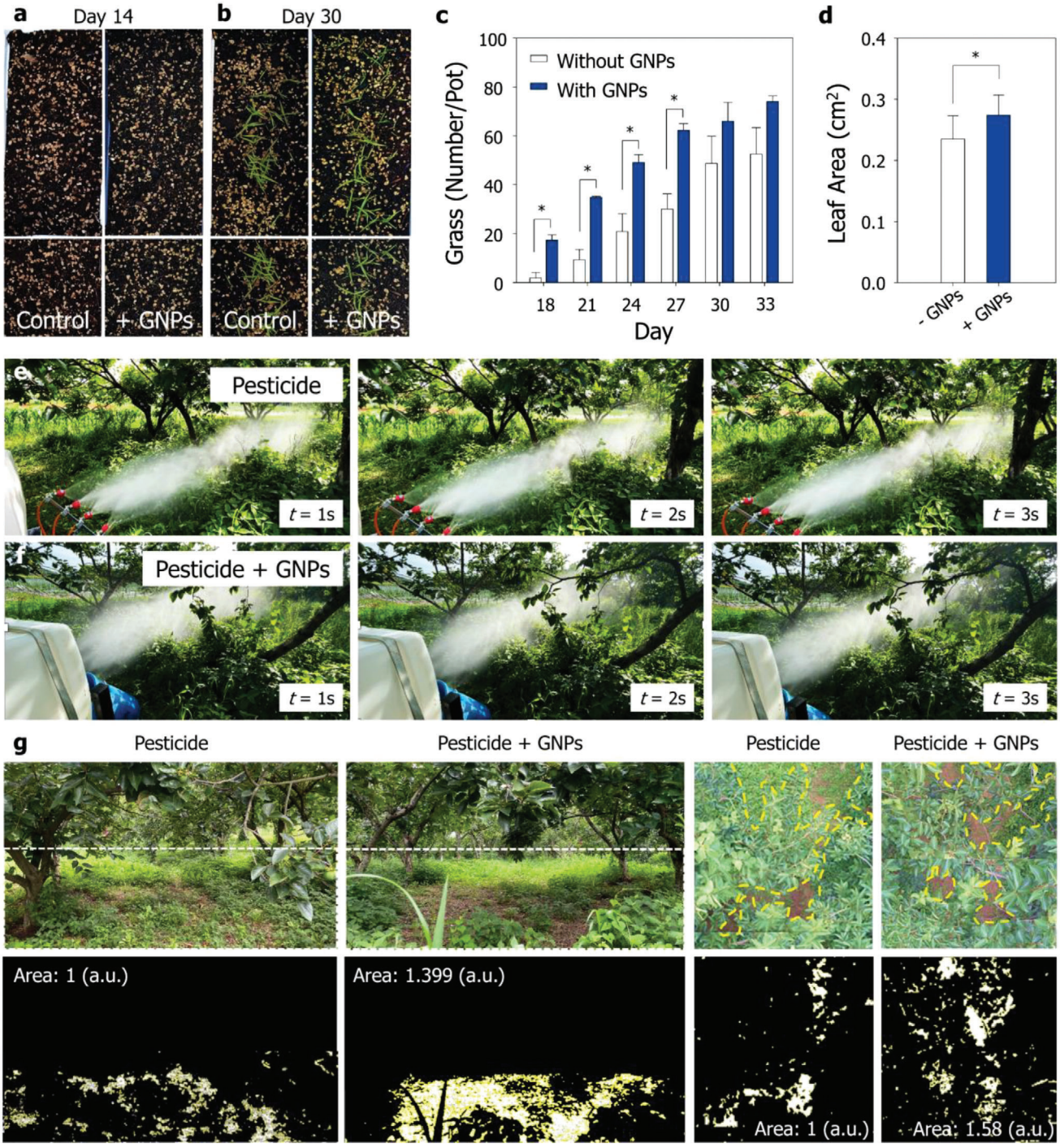

Figure 5. Applications of biocompatible gelatin nanoparticles (GNPs) on plant growth and weed killing effects. a and b) Representative photographs of grass in the soil with and without GNPs at day 14 and day 30. c) Quantification of the time-dependent grass germination in the soil with and without GNPs for 1 month. Data were analyzed by Student's *t* test (* $P < 0.05$). d) Quantification of grass leaf area at 30 days. Data were analyzed by Tukey tests (* $P < 0.05$). e) Representative photograph of spraying of pesticide using a pest control machine in a real farm. f) Representative photograph of spraying of pesticide with gelatin using a pest control machine in a real farm. g) Representative photographs and soil part extracted images of the real farm (side and upper side) 2 months after spraying of pesticide with and without GNPs. Error bars represent the standard deviation of means (n = 3 per group). Data were analyzed by one-way analysis of variance (*$P < 0.05$).

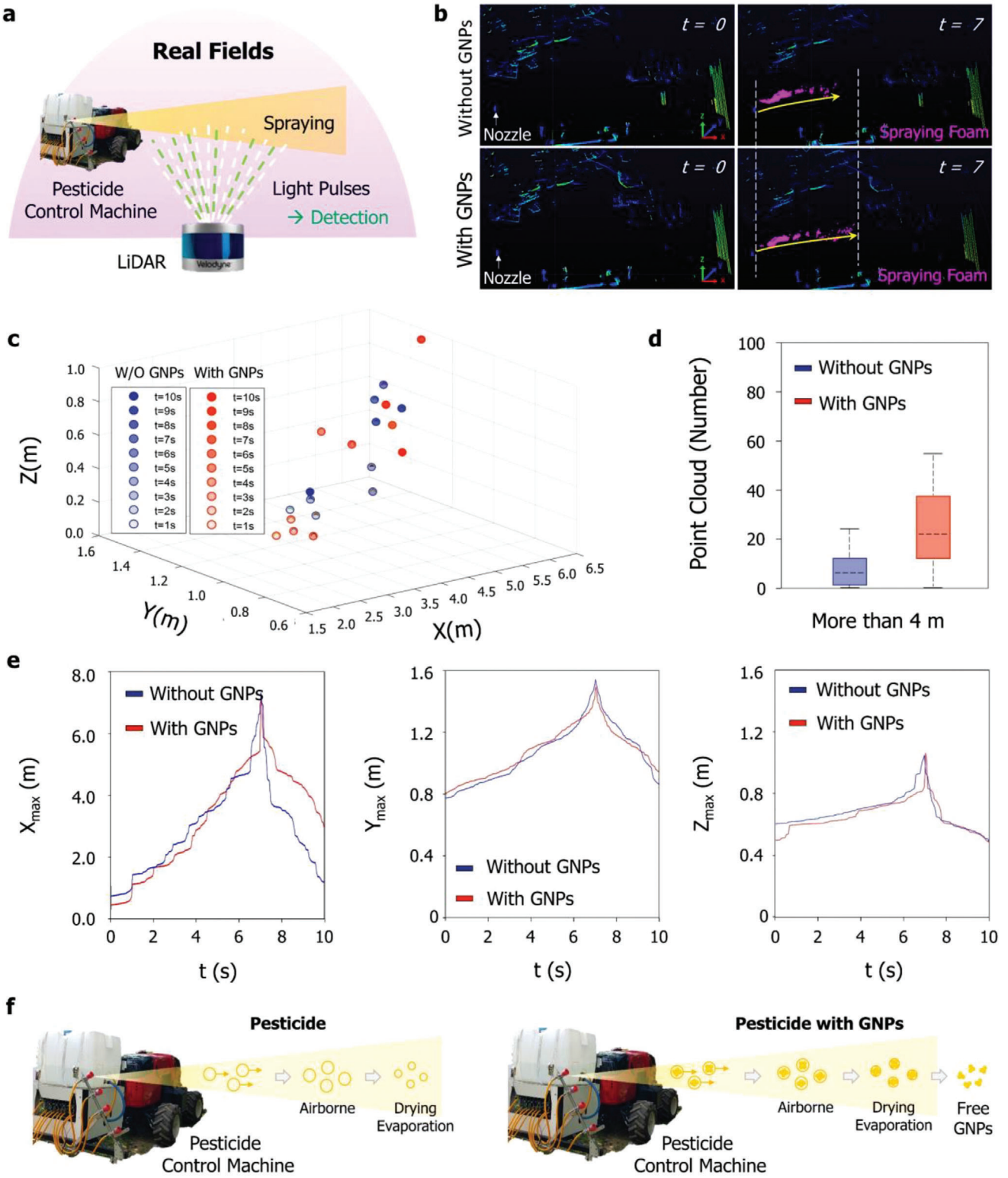

Figure 6. Enhanced spraying form of model pesticides with biocompatible gelatin nanoparticles (GNPs). a) Schematic of LiDAR-based spraying form detection. The object, including droplets from the nozzle, are detected by the light pulses. b) Representative point cloud images of spraying form with/without GNPs at 0 and 7 s. The droplets are shown as pink points. c) Quantification of the time-dependent maximum point cloud of droplets with/without GNPs. d) Quantification of point cloud number exceeding the threshold set to 4 m. e) Quantification of time-dependent maximum point clouds of droplets with/without GNPs according to the axis. f) Summarization of the finding of LiDAR-based droplet with/without GNPs. Error bars represent the standard deviation of means (n = 10 per group). Data were analyzed by one-way analysis of variance (*P < 0.05).

(Figure 6b). The time-dependent average of the maximum point cloud of droplets with/without GNPs is shown in Figure 6c. The range varied according to the presence of GNPs, in which droplets with GNPs tended to spread further over time, whereas droplets without GNPs showed weaker spreading than droplets with GNPs. Analyzing Figure 6c in more detail demonstrates that the range of droplets expanded at ≈4 m. Therefore, we compared the point cloud of droplets with and without GNPs at more than 4 m. The number of point clouds could explain a substantial amount of the difference between the groups; that is, the droplets with GNPs further spread into the injector nozzle orientations, indicating that GNPs might affect the maintenance of droplets in the air (Figure 6d). To confirm the specific distribution of droplets along the axis, the time-dependent maximum cloud point was evaluated (Figure 5e). The maximum cloud points of the y and z axes were similar between droplets with and without GNPs. However, the x-axis (representing injector nozzle orientations) demonstrated that the droplets were maintained in the air and further spread on the axis for ≈3 s longer in GNPs group. Hagendorfer et al. confirmed that smaller droplets with solid nanoparticles under 200 nm were released in the air, and then the water droplets evaporated and dried, whereas nanoparticles below 100 nm remained in the air.[73] Following these findings, we summarized the effects of GNPs on spraying form in Figure 6f.

3. Discussion: Unveiling the Versatility of GNPs for Sustainable Agriculture

We demonstrated the potential application of engineered GNPs for sustainable agriculture using plant, crops, and insect pest models. Specifically, GNPs improved the attachment of agrochemicals to the leaf surface regardless of the surface, and the loaded chemicals exhibited sustainable release. These useful effects are attributed to the nanometer size, positively charged surface property, and swelling behavior of gelatin. Ha et al. revealed the adsorption and dispersion of nanoparticles on leaf surfaces.[74] The sedimentation effect is relatively weaker than the internal convective flow effect, which can promote the accumulation of nanoparticles near the drops on leaf surfaces instead of initially penetrating through the stomatal pathway. This rapidly transforms to the wetted "Wenzel state" and the nanoparticles are attached on the microstructures of the leaf surfaces by water evaporation. The swelling behavior of GNPs was affected by the cross-link density because gelatin contains diverse chemical groups that enable covalent cross-linking with gelatin, which promotes the loading and diffusion of the drug.[75]

To our knowledge, this is the first attempt at using biocompatible nanoparticle (i.e., GNPs) in agricultural application, demonstrating their unique abilities to regulate the fate of plants, crops, and insects as desired by modifying the blending procedure. After the treatment of a model plant (*Arabidopsis*) and crop (*Camelina sativa*) with GNPs for 14 and 10 days respectively, no toxicity was observed in any form and also improved the plant growth due to the presence of amino acids in GNPs which act as signal molecules, regulating root and shoot architecture.[76] Previous studies have shown the impact of bioengineered gelatin on plant growth and soil condition, whereas others have demonstrated their cytotoxicity to plant and environment systems.[49,77] When GNPs are applied in plant, it was adsorbed on the surfaces of the plant root without the prevention of adsorption of the other nutrients (Figure 2j). Through gene expression analysis, the various root growth-related gene increased with the treatment of GNPs. It is revealed that Auxin accumulation can promote lateral root growth and development, and PIN-mediated auxin transport is regarded as an important regulator to increase Auxin accumulation. Our data showed increased PIN-related gene (Figure 2k), and it might be accelerated the lateral root growth.[78] In addition, the biocompatible particles can retain the healthy microbial activity in the soil, which is important factor in the maintenance of soil fertility.[79] GNPs were not affected on antibacterial effects (Figure S3a, Supporting Information), showing no bacteria zone of inhibition. These finding demonstrates that raw GNPs were not cytotoxicity to plant and microorganism in agricultural fields, and it was not inhibiting the activity of the plant and bacteria in the soil.

GNPs with agrochemical materials could more potently disturb the functions of insect pests and weeds than the agrochemicals alone. This could be due to the ability of GNPs to retain the active ingredient (i.e., pesticide and herbicide) on the surfaces of leaves. Moreover, i-GNPs showed increased insecticidal effects than the pure insecticide, whereas there were no differences between groups at a lower insecticide concentration, indicating the need to optimize the pesticide concentration when applying GNPs to agricultural fields. Thus, we fabricated i-GNPs and h-GNPs using commercial agrochemical materials (1:1 = GNPs:insecticide/herbicide, 0.03 g L^{-1}) in this study, which is the recommended concentration of a commercial pesticide.

Yeguerman et al. developed essential oil-loaded polymeric nanoparticles to control the German cockroach, which had sublethal effects by negatively affecting the nutritional indices (reduced food consumption and the efficiency of ingested food conversion), thereby inhibiting the growth rate.[80] We confirmed that the number of killed larvae with i-GNPs was higher than that under-insecticide treatment after washing. This effect was related to a reduced mass rate among i-GNPs-treated larva (Figure 3d), confirming inhibition of food consumption and the efficiency of food conversion. Thus, this nutritional reduction could be due to the change of enzymatic systems related to digestion and food adsorption by the indirect effect of polymeric nanoparticles (i.e., GNPs).[81] By contrast, the efficiency of the h-GNPs to kill the weeds can be explained by a direct effect. Interestingly, there was no difference in the early stage (≈1 week), but the h-GNPs had a sustained killing effect on weeds, which exhibit high resistance. Commercial herbicide can control growth, photosynthesis, amino acid synthesis, and seedlings. Weeds with such inhibited functions show symptoms, including leaf/stem malformation (e.g., curled, twisted, crinkled structure of leaf and stem), changed leaf color, root damage, and pigmentation. According to our results, the leaf color of weeds changed to yellow and then to brown after h-GNP treatment. The representative sequence of symptoms for killing weeds is as follows: yellowing of the leaf veins, yellowing of the leaf margins, turning to brown, inhibition of photosynthesis, and death. This process indicates that the herbicide only affected the leaves without its transportation inside the plant. Although further studies are needed to fully understand the underlying molecular mechanisms, the unique properties of GNPs may indeed influence the performance of herbicides. One possible mechanism is the enhanced adhesion

and retention of the herbicide on plant surfaces. This property helps prevent the loss of the pesticide due to rainfall or irrigation, thereby increasing its contact time with weeds and improving herbicidal activity (Figure S7a, Supporting Information). Yu et al., investigated nanoparticle-based adhesion to enhance the foliar retention, and they demonstrated that the H_2N-based nanoparticles exhibited better adhesion capabilities compared to other nanoparticles (i.e., CH_3CO- and HOOC-based nanoparticles), highlighting the strong interaction between foliage and nanoparticles through hydrogen bond, electrostatic attraction, and covalent bond.[82] A second possible mechanism is controlled release, which provides a sustained release of the active ingredient over time. Figures S1 and S2b (Supporting Information) in our study show the release kinetics under various conditions including different concentration and temperature, demonstrating sustained release behavior regardless of these conditions. Notably, the release percentage of urea at 0.06 g mL^{-1} GNPs concentration was the highest, attributed to the increased urea concentration interfering with the formation of hydrogen bonds (H-H), consequently reducing the risk of further urea entrapment within the loosely constructed inner structure of GNPs.[71] The pesticide-loaded GNPs were attached to the leaves, then the active ingredient of pesticides may be released gradually, prolonging the herbicidal effect and improving weed control. A third possible mechanism involves targeted delivery of herbicide-loaded GNPs. GNPs can be functionalized to specifically target weeds or weed-prone areas, delivering the pesticide directly to the intended target. In our study, the developed GNPs exhibited high attachability to targeted leaf site. Additionally, their whistle capacity increased attachment to different sites, such as upper and bottom leaves. This targeted delivery approach minimizes off-target effects and increases the efficiency of herbicide performance.

In addition, we confirmed the effect of GNPs at the field level, which improved plant (grass) growth and the pesticide (herbicide) effect. Through the LiDAR system, we confirmed the different spraying forms of the solution with and without GNPs. Via the strong pressure of the pesticide control machine, the solution with GNPs was sprayed into the air, and the large water droplets with GNPs directly fell off. By contrast, the small water droplets with GNPs were dispersed in the air, and free GNPs were maintained in the air after water evaporation in the solution. Nazarenko et al. reported that spraying engineered nanoparticles were affected by the sprayer type, and Hagendorfer et al. revealed that nanoparticles with an aerosol condition induced by a gas sprayer were more dispersed than those delivered via a hand sprayer.[73,83] Our finding of differences in the spraying form suggests a new role of nanomaterial-based delivery in field applications. Specifically, a nanoparticle-based solution might be widely sprayed with smaller droplets by high pressure or by varying the spraying type.

3.1. Economic Assessment of GNPs and Future Suggestions

The current conditions and cost for GNPs production are relatively straightforward and low. GNPs are small polymer-based nanoparticles synthesized from gelatin powder (type A) in the laboratory using acetone and glutaraldehyde, with the process spanning various temperature ranges over 12 h. The estimated cost of GNPs production and application in crop cultivation is ≈USD 2220.25. This figure includes variable costs of fabrication, chemical fertilizers, pesticides, seeds, land and machinery rent, and miscellaneous expenses. If GNPs were produced on a large scale in the agrochemical industry, the cost may initially increase due to additional procedures and materials required for industrial-scale production. However, significant cost reductions can be achieved by optimizing the fabrication process to minimize the use of expensive chemicals, exploring alternative raw materials, and scaling up production to benefit from economies of scale. Additionally, enhancing application efficiency through advanced delivery methods could further contribute to lowering costs. Large-scale industrial production has the potential to further reduce costs to ≈USD 500–1000 by optimizing the synthesis process, reducing labor and land costs, and minimizing the need for specialized equipment. This would make GNPs more economically feasible for widespread agricultural use, providing a cost-effective solution for enhancing plant growth and nutrient absorption.

4. Conclusion

While there is a wealth of literature on the use of nanomaterials/particles for plant and crop growth, their application in real agriculture still faces numerous limitations that require further research. To better harness their potential efficiency, we have developed gelatin nanoparticles (GNPs) as a versatile tool to enhance plant growth and maintain pesticide efficacy. GNPs possess unique characteristics such as uniformity in the nanoscale, positively charged surfaces, and high loading capacity, enabling them to readily attach to plant leaves regardless of their hydrophobic or hydrophilic properties. In our study, we proposed two different roles for GNPs in agricultural fields. First, using a plant model, we confirmed the effectiveness of GNPs in promoting *A. thaliana* growth, as evidenced by phenotypic and genotypic changes such as increases in root length, leaf area, leaf number, and expression of root growth-related genes. Second, we demonstrated that the combination of GNPs and pesticides can enhance pesticide efficacy, with GNPs carrying insecticide promoting insecticidal effects and GNPs carrying herbicide increasing weed killing effects. Importantly, GNPs can be applied using a simple spraying technique in real agricultural workplaces, with similar results obtained as in laboratory conditions, indicating their potential for practical use. While further studies are required to elucidate the underlying molecular mechanisms of GNPs' effects at the field level, our study provides conceptual evidence for their application in agriculture. We believe that biocompatible GNPs, with/without pesticides, could serve as a nano-platform for engineering plant and insect pest functions, ultimately contributing to sustainable agriculture.

5. Experimental Section

Fabrication of GNPs: GNPs with stable size distribution were fabricated by the conventional two-step desolvation method.[28] Specifically, gelatin powder (type A, Sigma–Aldrich, St. Louis, MO, USA) was dissolved in 25 mL of warm deionized water (5.0% w/v) under 50 °C heating and stirring. Twenty-five milliliters of acetone were directly poured into the dissolved gelatin solution, and the sediment with a high molar mass of gelatin

was redissolved in 25 mL of warm deionized water under 50 °C heating and stirring. The pH of the solution was adjusted to pH 3 using HCl, and 75 mL of acetone was slowly added with stirring at 600 rpm and 40 °C for 1 h. The solution became milky with the addition of ≈60 mL acetone, which was stirred at 4 °C in a cold laboratory chamber for 1 h. Then, 280 µL of glutaraldehyde (25%, v/v) as cross-linker was gradually added into the solution, which was stirred at 4 °C in a cold laboratory chamber overnight. Under centrifugation (4 °C and 6500 rpm), the gelatin nanoparticles were washed with 75% acetone three times, and the centrifugated GNPs were lyophilized for 4 days.

Characterization of the Fabricated GNPs: The morphology of the fabricated GNPs was confirmed using a JSM-7500F field-emission scanning electron microscope (FE-SEM, JEOL Ltd., Tokyo, Japan). SEM images (n = 5) were used to determine the size distribution of GNPs by multi-point function in image J software (National Institutes of Health, Bethesda, MD, USA). The chemical properties were analyzed by FT-IR spectroscopy (Spectrum 400). GNPs was reacted with pesticide solution for more 2 h, and pesticide -loaded GNPs was inverted at 20 rpm in a 36 °C incubator, and it was measured by an FT-IR spectroscopy.

The zeta potential of GNPs and average diameter of GNPs in pesticide solution were measured by a zeta-potential and particle size analyzer (n = 3, ELSZ-2000, Otsuka Electronics Co., Ltd., Osaka, Japan) and the mechanical properties were analyzed with an MCT 1150 system (AND, Korea). For the drug release test, trypan blue was used as the model drug. GNPs at 0.03 g were reacted with a 0.015, 0.03, or 0.06 g mL^{-1} trypan blue solution and cured for 2 h at room temperature. The trypan blue-loaded GNPs was inverted at 20 rpm in a 4, 18, and 36 °C incubator, and the released trypan blue solution was measured by an UV–vis spectrophotometer at 595 nm absorbance (iMark Microplate Reader; Bio-Rad, Hercules, CA, USA).

Loading Efficiency Analysis: For uploading efficiency of urea, a UV–vis spectrophotometer (Model T60, PG Instruments, UK) was used the amount of urea uploaded from the solution into the GNPs was calculated.[48] For determining the urea loading a 0.03 g of GNPs incubated in various concentrations of urea (0.015, 0.03, and 0.06 g mL^{-1}) at room temperature for 3 h in order to release the urea. An equal number of blank GNPs (0.03 g) (i.e., containing no urea) was also incubated at room temperature for 3 h. After this, gently centrifuged this filtrate at 10 000 rpm for 3 min. The supernatant is collected and given a 10-min reaction with *p*-dimethylamine benzaldehyde before the sample is run through a spectrophotometer. The solution's absorbance was then measured using a UV-spectrophotometer (iMark Microplate Reader; Bio-Rad, Hercules, CA, USA) at 420 nm wavelength. The absorbance of the supernatant obtained from the blank GNPs was subtracted and the concentration of urea was determined by comparison to the absorbance of a set of standards.

For Release Kinetic Analysis: Urea was used as a model fertilizer to evaluate the fertilizer release profile of the GNPs. In brief, the GNPs were impregnated with a 0.05, 0.03, and 0.06 g mL^{-1} solution of urea at a ratio of 5 µL mg^{-1} and cured for 2 h at room temperature. GNPs were immersed in phosphate-buffered saline at a ratio of 1.5 mL/5 mg and then inverted at 20 rpm in a 37 °C incubator. The urea concentration in the supernatant was determined by measuring the absorbance at 420 nm using a UV-spectrophotometer (iMark Microplate Reader; Bio-Rad, Hercules, CA, USA).

SEM Imaging of GNPs-Treated Plants: GNPs was confirmed using a JSM-7500F field-emission scanning GNPs were dispersed in deionized water (0.03 g of GNPs/100 mL water), and treated onto fresh taro and lettuce leaves at a distance of 30 cm (0.24 g of GNPs solution – 1 spray). The surfaces of the leaves were washed with pure deionized water once or twice after the surface was dry. *Arabidopsis thaliana L*. were separately cultured on agar plates with and without GNPs for 2 weeks. Thereafter, all samples, including taro, lettuce leaves, and *A. thaliana*, were carefully separated from the nutrient medium, fixed with 4% paraformaldehyde (Sigma–Aldrich) for 10 min, and then washed three times with 1× phosphate-buffered saline (PBS). The fixed samples were reacted with 1% osmium tetroxide (Sigma-Aldrich) for 1 h, washed three times with 1× PBS, and dehydrated using a graded series of ethanol solutions (30%, 50%, 70%, 80%, 90%, and 100% v/v). The samples were coated with a Pt layer (≈5 nm thick) by metal sputtering, and images were obtained using JSM-7500F FE-SEM (JEOL Ltd.).

Preparation of GNP Nutrient Medium and Evaluation of Plant Growth: Murashige and Skoog (MS) nutrient medium containing 2.2 g of MS nutrient, 10 g of agar (DUCHEFA, Haarlem, The Netherlands), 0.5 g of 2-(N-morpholino) ethane sulfonic acid powder (Sigma–Aldrich, St. Louis, MO, USA), and 30 g of sucrose was added to the GNP solution (GNP: water = 0.03 g: 1L) with stirring. The pH of the prepared solution was adjusted to 5.6–5.8. The MS medium with GNPs (GNPs/MS medium) was sterilized in an autoclave (DH18CAT00210081; Daihan Scientific) and dried in a biosafety hood under a sterilized condition before use. Seeds of *A. thaliana* were surface sterilized with 70% ethanol and 20% sodium hypochlorite and then treated with MS medium at 4 °C in the dark for stratification. After three days, the germinated seeds were transferred to MS medium and GNPs/MS medium and left to grow at 24 °C. Each germination assay (n = 4) was carried out using 90–100 seeds. To determine the effects of GNPs on plant seedling growth, the root length, leaf area, fresh weight, and leaf number of the seedlings were measured at 3 and 10 days after growth on MS medium and GNPs/MS medium.

Preparation of MS Medium having N, with and without GNPs and Evaluation of Plant Prowth: Murashige and Skoog (MS) nutrient medium containing 0.33 g of MS nutrient, 1.05 g of agar (DUCHEFA, Haarlem, The Netherlands), and 4.5 g of sucrose as a control group and same MS medium along with nanomaterial solution (GNP: water = 0.03 g: 150 mL) was prepared with stirring. The pH of the prepared solutions were adjusted to 5.6–5.8. The MS medium (as control) and MS medium with nanomaterials (NPs/MS medium) was sterilized in an autoclave (DH18CAT00210081; Daihan Scientific) and dried in a biosafety hood under a sterilized condition before use. Seeds of Arabidopsis were surface sterilized with 70% ethanol and 30% sodium hypochlorite and then treated with MS medium at 4 °C in the dark for stratification. After two days, the germinated seeds were transferred to MS medium and GNPs/MS and left to grow at 24 °C. Each germination assay (n = 3) was carried out. To determine the nano fertilizer property of GNPs on plant seedling growth, the root length, leaf area, fresh weight, and leaf number of the seedlings were measured at 3 and 10 days after growth on MS medium and GNPs/MS.

Preparation of GNP-Nutrient Medium and Evaluation of Plant Growth: Murashige and Skoog (MS) nutrient medium containing 0.33 g of MS nutrient, 1.05 g of agar (DUCHEFA, Haarlem, The Netherlands), and 4.5 g of sucrose was added to the nanomaterial solution (GNP: water = 0.03 g: 150 ml) with stirring. The pH of the prepared solutions were adjusted to 5.6–5.8. The MS medium with nanomaterials (NPs/MS medium) was sterilized in an autoclave (DH18CAT00210081; Daihan Scientific) and dried in a biosafety hood under a sterilized condition before use. Seeds of *Camelina sativa* were surface sterilized with 70% ethanol and 30% sodium hypochlorite and then treated with MS medium at 4 °C in the dark for stratification. After two days, the germinated seeds were transferred to MS medium and GNPs/MS and left to grow at 24 °C. Each germination assay (n = 3) was carried out. To determine the potential effects of NPs for fertilizer delivery on plant seedling growth, the root length, leaf area, fresh weight, and leaf number of the seedlings were measured at 3 and 10 days after growth on MS medium and GNPs/MS. Sterile Magenta boxes were used for all germination experiments.

Preparation of Nanomaterials-Nutrient Medium and Evaluation of Plant Growth: Murashige and Skoog (MS) nutrient medium containing 0.33 g of MS nutrient, 1.05 g of agar (DUCHEFA, Haarlem, The Netherlands), and 4.5 g of sucrose was added to the nanomaterial solution (GNP: water = 0.03 g: 150 ml; GO: water = 100 µg: 150 ml; PCN-224: water = 100 µg) and urea (CAS-No: 57-13-6, Germany) with stirring. The pH of the prepared solutions were adjusted to 5.6–5.8. The MS medium with nanomaterials (NPs/MS medium) was sterilized in an autoclave (DH18CAT00210081; Daihan Scientific) and dried in a biosafety hood under a sterilized condition before use. Seeds of *Camelina sativa* were surface sterilized with 70% ethanol and 30% sodium hypochlorite and then treated with MS medium at 4 °C in the dark for stratification. After two days, the germinated seeds were transferred to NPs/MS medium and left to grow at 24 °C. Each germination assay (n = 3) was carried out. To determine the potential effects of NPs for fertilizer delivery in *Camelina sativa* seedling growth, the root length, leaf area, fresh weight, and leaf number of the seedlings were

measured at 3 and 21 days after growth on NPs/MS medium. Sterile Magenta boxes were used for all germination experiments.

Chlorophyll Content Analysis: The determination of chlorophyll contents was performed by taking total of 50 mg of leaves from all samples were ground on ice with 10 ml 95% ethanol (v/v). Then, the extracts were filtered and brought to a volume of 25 ml using 95% ethanol (v/v). Finally, the chlorophyll extracts were analyzed using a UV-spectrophotometer (iMark Microplate Reader; Bio-Rad, Hercules, CA, USA). The absorbance readings were performed at 665 nm absorbance. All analyses were repeated three times.

Plant Gene Array: To confirm the expression of root growth-related genes, reverse transcription-quantitative polymerase chain reaction (RT-qPCR) was performed. Briefly, mRNA was separated into 300-nucleotide-long fragments in an RNA fragmentation buffer (10 mM Tris-HCl, pH 7.0, 10 mM $ZnCl_2$). The prepared RNAs and immunoprecipitated RNAs were reverse-transcribed by reverse transcriptase with random hexamer primers, and the levels of each transcript were measured using q PCR performed on a Rotor-Gene Q thermal cycler (Qiagen, Hilden, Germany) with a SYBR Green PCR kit (Qiagen, Hilden, Germany) and gene-specific primers listed as follows:

Primer name	Forward	Reverse
PLT1	TGCAGTGACCAACTTCGAGATC 3′	GGAAACTTGAACCAAGGGCTAT 3′
PLT2	GCACTTAAATATTGGGGTCCCT 3′	ATCCTTGCTTGCCATCTTCC 3′
PIN1	ACATAAGCAACAAAACGACGCA 3′	CACTTGAAGGAAATGAGGGACC 3′
PIN2	ACATAAGCAACAAAACGACGCA 3′	CACTTGAAGGAAATGAGGGACC 3′
PIN3	TGGCATCCTCCCCGAGAT 3′	CCGCCCGTTGGAAGAGTC 3′
PIN7	TCCACAGCAGAGCTAAACCCTA 3′	AAGCAACAAGAGCCCAAATGA 3′
ARR1	ACGGTGGTTCAGTGAGGGTG 3′	CGATGGAGTATGCGTCAAAGTC 3′
ARR2	CGCAGCATTTTCCACTTCG 3′	TCACTGTCTCCGCCACTCTTT 3′
ARR7	ACGGATTACTCAATGCCAGGAC 3′	GCTAGCTTCACCGGTTTCAAC 3′
CRF2	AATGGGCGGCGGAGATAA 3′	GACGGTGGTGGGGCTTTC 3′
CRF3	GTCGAGTCGTCAACGTCCTAAT 3′	CGCCGTCTCAAAAGTCCC 3′
CRF7	AGTGGGCGGCTGAGATTAGA 3′	GCAGAATCAACATCAGGACGG 3′
AUX1	TCGGAAGGAGTAGAAGCGATAG 3′	AAGCGTCCCAGACAGAGCC 3′
SHY2	GGGATTACCGGGAACAGATAAT 3′	CTGAGCCTTTCGAGGAGGG 3′
IAA16	ATCACGGAGGAGAAATGGCT 3′	CTTGGCTGGTGGTTTTACGA 3′
DR5	AAGCATTCTGGGCAGGAGC 3′	CCTTCGTTCAGAGCCGTCAC 3′
WOX5	GATCTGTTTCGAGCCGGTCT 3′	GGAGATTTTACGACGTTTCTGC 3′

In Vivo Insect Study: Aphis gossypii (n = 50, third insta) was collected from chili pepper plant and cabbage white butterfly caterpillars (*Pieris rapae*, third insta, n = 5) were purchased from WANI Science (Seoul, Korea). The diluted insecticide solution (Setis, Farmhannong, Seoul, Korea) was reacted with/without gelatin nanoparticles (0.015 and 0.03 g) for more 2 h without any solvent. The insects were grown with leaves, and diluted insecticide solution with/without GNPs was treated to samples for 1 time and dried before insect culture. The insect with samples were sealed to limit the external effect in a dish. It was reared at a temperature of 27 °C, with a relative humidity ranging from 70% to 80%, and a photoperiod of 16 h of light followed by 8 h of darkness. To confirm the remained insecticide effects with gelatin nanoparticles, pure DI water was treated using spray for 20 times. The killed insect number and insect mass were recorded every day.

Aphis gossypii study (water 1L)	
Pesticide 0.03 g + GNPs 0 g	Pesticide 0.015 g + GNPs 0 g
Pesticide 0.03 g + GNPs 0.015 g	Pesticide 0.015 g + GNPs 0.0075 g
Pesticide 0.03 g + GNPs 0.03 g	Pesticide 0.015 g + GNPs 0.015 g

Butterfly caterpillars study (water 1L)	
Pesticide 0.03 g + GNPs 0 g	Pesticide 0.03 g + GNPs 0.015 g
Pesticide 0.03 g + GNPs 0.03 g	

In Vivo Weed Study: The weeds on the ground were used for the killing effects of the herbicide (0.03 g L^{-1}; Terado, Farmhanong, Seoul, Korea) with/without gelatin nanoparticles (0.03 g), which was reacted for more 2 h. The chemical name of Terado is Tiafenacil, and its empirical formula is $C_{19}H_{18}ClF_4N_3O_5S$. Tiafenacil (Terrad'or), exhibiting low oral and dermal acute toxicity, classified as Grade 5. It could be used as effective herbicide to control diot and monocot weeds.[84] The herbicide solution was treated using spray (1 spraying = 200 µL, 10 times) over an area of 0.12 m^2 (30 × 40 cm), and the images were collected every day. The images were quantified by multi-point function in image J software (NIH, Bethesda, MD, USA).

Rain-Fastness Test: The fertilizer used in this experiment was urea (0.03 g mL^{-1}, suspension concentrate). For determining the urea retention ability, 2 ml suspension of each group (urea and GNPs-urea) was sprayed on *Camelina sativa* leaves (14-day seedlings) and left to incubate at room temperature for 0.5–1 h. The leaves were fixed to a glass slide at 45° and then washed with deionized water at a flow rate of 1.5 mL min^{-1} from a height of 20 cm for 4 min. The eluents were collected and the content of urea in the eluates was measured with a UV–vis spectrophotometer (iMark Microplate Reader; Bio-Rad, Hercules, CA, USA) at 420 nm. The rain-fastness was calculated based on the equation $R_f = (m - m_a)/m \times 100\%$, where m is the mass of urea on the leaves before washing and m_a is the mass of urea in the eluate. Each test was conducted in three replicates.

Field Experiment: A pesticide control machine-based field experiment was conducted at a persimmon orchard in Bonghwang, Naju, Republic of Korea. The pesticide control machine was composed of a pesticide tank, flow rate control unit, pulse width modulation solenoid valves, and nozzles, and spraying was controlled using the flow rate control unit. The pesticide solutions (10 L) with or without 0.3 g GNPs were prepared in the pesticide tank and were sprayed out of reach of the persimmon leaves for 10 s. After 2 months, field images were obtained using a 3 DR Solo Quadcopter (B&H Foto&Electronics Corp., NY, USA).

Spraying Form Detection using LiDAR: Sprayed droplets from the pesticide control machine were obtained as point cloud data using LiDAR (Puck, Velodyne Lidar, CA, USA) for 10 s, and the outer surface of an object was measured into the point by 3D LiDAR photogrammetry software (Veloview, CA, USA). An obtained point cloud creates a 3D shape, and each point position has a set of Cartesian coordinates (x, y, z). The spraying form was separated into the specific point cloud through the set of the region of interest, and each point cloud was calculated by MATLAB (MathWorks, MA, USA). To verify the effect of nanomaterials on spraying distance, the threshold was set to over 4 m, which was close to the maximum distance of spraying. Separated point clouds were defined as:

$$p\ (a_1,\ a_2,\ \ldots,\ a_n) = \sum p_{sf} = \sum_{a \in p_{st}} p_a + \sum_{b \in p_{st}} p_b \quad (1)$$

where p_a is a point cloud of less than the threshold (i.e., <4 m) and p_b is point cloud of more than the threshold (i.e., >4 m).

Statistical Analysis: Student's t-test was used to compare data between two different conditions. To compare three or more conditions, one-way

analysis of variance was performed. In all cases, P values of less than 0.05 were considered statistically significant. All quantitative results are presented as the mean ± standard deviation.

Supporting Information

Supporting Information is available from the Wiley Online Library or from the author.

Acknowledgements

S.P. and M.S. contributed equally to this work. This work was supported by the Korea Institute of Planning and Evaluation for Technology in Food, Agriculture and Forestry (IPET) through the Agriculture, Food and Rural Affairs Research Center Support Program, funded by the Ministry of Agriculture, Food and Rural Affairs (MAFRA) (Project No. 714002). This work was also supported by Korea Institute of Planning and Evaluation for Technology in Food, Agriculture and Forestry (IPET) through the Agriculture and Food Convergence Technologies Program for Research Manpower development, funded by Ministry of Agriculture, Food and Rural Affairs (MAFRA) (project no. RS-2024-00397026); Regional Innovation Strategy (RIS) through the National Research Foundation of Korea (NRF) funded by Ministry of Education (MOE) (2021RIS-002); National Research Foundation of Korea (NRF) grant funded by Korea government (MSIT) (NRF-2022M3A9E4017151), and also supported by National Research Foundation of Korea (NRF) grant funded by the Korea government (MSIT) (NRF-2020R1A5A8018367). The authors were grateful to the Center for Research Facilities at the Chonnam National University for their assistance in the analysis of the properties of GNPs. (FE-SEM, FT-IR, and Raman analysis).

Conflict of Interest

The authors declare no conflict of interest.

Data Availability Statement

The data that support the findings of this study are available from the corresponding author upon reasonable request.

Keywords

agriculture, biocompatible nanoparticles, gelatin nanoparticles, pesticide effect, plant growth

Received: April 11, 2024
Revised: June 17, 2024
Published online: July 1, 2024

[1] G. V. Lowry, A. Avellan, L. M. Gilbertson, *Nat. Nanotechnol.* **2019**, *14*, 517.
[2] C. R. Kagan, *ACS nano* **2016**, *10*, 2985.
[3] P. Abhilash, V. Tripathi, S. A. Edrisi, R. K. Dubey, M. Bakshi, P. K. Dubey, H. Singh, S. D. Ebbs, *Energy Ecol. Environ.* **2016**, *1*, 54.
[4] M. Safdar, W. Kim, S. Park, Y. Gwon, Y.-O. Kim, J. Kim, *J. Nanobiotechnol.* **2022**, *20*, 275.
[5] P. Shrivastava, R. Kumar, *Saudi J. Biol. Sci.* **2015**, *22*, 123.
[6] C. Athanassiou, N. Kavallieratos, G. Benelli, D. Losic, P. Usha Rani, N. Desneux, *J. Pest Science* **2018**, *91*, 1.
[7] P. Deshpande, A. Dapkekar, M. D. Oak, K. M. Paknikar, J. M. Rajwade, *Carbohydr. Polym.* **2017**, *165*, 394.
[8] D. Goulson, *J. Appl. Ecol.* **2013**, *50*, 977.
[9] Food, Nations, A. O. o. t. U., The future of food and agriculture: Trends and challenges. Fao, **2017**.
[10] N. Mitter, K. Hussey, *Nat. Nanotechnol.* **2019**, *14*, 508.
[11] T. T. S. Lew, R. Sarojam, I.-C. Jang, B. S. Park, N. I. Naqvi, M. H. Wong, G. P. Singh, R. J. Ram, O. Shoseyov, K. Saito, *Nat. Plants* **2020**, *6*, 1408.
[12] T. Hofmann, G. V. Lowry, S. Ghoshal, N. Tufenkji, D. Brambilla, J. R. Dutcher, L. M. Gilbertson, J. P. Giraldo, J. M. Kinsella, M. P. Landry, *Nat. Food* **2020**, *1*, 416.
[13] P. Zhang, Z. Guo, Z. Zhang, H. Fu, J. C. White, I. Lynch, *Small* **2020**, *16*, 2000705.
[14] J. Fischer, S. J. Beckers, D. Yiamsawas, E. Thines, K. Landfester, F. R. Wurm, *Adv. Sci.* **2019**, *6*, 1802315.
[15] S. Park, H.-H. Park, K. Sun, Y. Gwon, M. Seong, S. Kim, T.-E. Park, H. Hyun, Y.-H. Choung, J. Kim, *ACS Nano* **2019**, *13*, 11181.
[16] Z. Yang, J. Tian, Z. Yin, C. Cui, W. Qian, F. Wei, *Carbon* **2019**, *141*, 467.
[17] N. Dasgupta, S. Ranjan, D. Mundekkad, C. Ramalingam, R. Shanker, A. Kumar, *Food Res. Int.* **2015**, *69*, 381.
[18] K. Poddar, J. Vijayan, S. Ray, T. Adak, in *Biotechnology for sustainable agriculture*, Elsevier Woodhead Publishing, Amsterdam **2018**, pp. 281–303.
[19] J. P. Giraldo, M. P. Landry, S. M. Faltermeier, T. P. McNicholas, N. M. Iverson, A. A. Boghossian, N. F. Reuel, A. J. Hilmer, F. Sen, J. A. Brew, *Nat. Mater.* **2014**, *13*, 400.
[20] A. Servin, W. Elmer, A. Mukherjee, R. De la Torre-Roche, H. Hamdi, J. C. White, P. Bindraban, C. Dimkpa, *J Nanopart Res* **2015**, *17*, 92.
[21] L. Zhao, L. Lu, A. Wang, H. Zhang, M. Huang, H. Wu, B. Xing, Z. Wang, R. Ji, *J. Agric. Food Chem.* **2020**, *68*, 1935.
[22] M. C. Camara, E. V. R. Campos, R. A. Monteiro, A. do Espirito Santo Pereira, P. L. de Freitas Proença, L. F. Fraceto, *J. Nanobiotechnol.* **2019**, *17*, 100.
[23] Q. Liu, B. Chen, Q. Wang, X. Shi, Z. Xiao, J. Lin, X. Fang, *Nano Lett.* **2009**, *9*, 1007.
[24] S.-Y. Kwak, J. P. Giraldo, M. H. Wong, V. B. Koman, T. T. S. Lew, J. Ell, M. C. Weidman, R. M. Sinclair, M. P. Landry, W. A. Tisdale, *Nano Lett.* **2017**, *17*, 7951.
[25] Y. Cao, E. Lim, M. Xu, J. K. Weng, B. Marelli, *Adv. Sci.* **2020**, *7*, 1903551.
[26] Y. Chai, C. Chen, X. Luo, S. Zhan, J. Kim, J. Luo, X. Wang, Z. Hu, Y. Ying, X. Liu, *Adv. Sci.* **2021**, *8*, 2003642.
[27] M. H. Wong, J. P. Giraldo, S.-Y. Kwak, V. B. Koman, R. Sinclair, T. T. S. Lew, G. Bisker, P. Liu, M. S. Strano, *Nat. Mater.* **2017**, *16*, 264.
[28] B. D. Cosa, W. Moar, S.-B. Lee, M. Miller, H. Daniell, *Nat. Biotechnol.* **2001**, *19*, 71.
[29] S.-Y. Kwak, T. T. S. Lew, C. J. Sweeney, V. B. Koman, M. H. Wong, K. Bohmert-Tatarev, K. D. Snell, J. S. Seo, N.-H. Chua, M. S. Strano, *Nat. Nanotechnol.* **2019**, *14*, 447.
[30] S. Park, Y. Jeon, T. Han, S. Kim, Y. Gwon, J. Kim, *Food Packag. Shelf Life* **2020**, *26*, 100570.
[31] H. Zhang, Y. Li, J.-K. Zhu, *Nat Plants* **2018**, *4*, 989.
[32] S. Park, K. S. Choi, S. Kim, Y. Gwon, J. Kim, *Nanomaterials* **2020**, *10*, 758.
[33] K. Pandey, M. Anas, V. K. Hicks, M. J. Green, M. V. Khodakovskaya, *Sci. Rep.* **2019**, *9*, 19358.
[34] F. Zhao, Y. Zhao, Y. Liu, X. Chang, C. Chen, Y. Zhao, *Small* **2011**, *7*, 1322.
[35] J. Kim, K. S. Choi, Y. Kim, K. T. Lim, H. Seonwoo, Y. Park, D. H. Kim, P. H. Choung, C. S. Cho, S. Y. Kim, *J. Biomed. Mater. Res. A* **2013**, *101*, 3520.
[36] C. A. Deutsch, J. J. Tewksbury, M. Tigchelaar, D. S. Battisti, S. C. Merrill, R. B. Huey, R. L. Naylor, *Science* **2018**, *361*, 916.
[37] I. Sathisaran, M. Balasubramanian, *Heliyon* **2020**, *6*.

[38] E. S. Juan-Martínez, M. Sandoval-Villa, L. I. Trejo-Téllez, Y. Jiménez-Flores, M. Á. Aguilar-Méndez, *Ingeniería agrícola y biosistemas* **2020**, *12*, 69.
[39] Y. Gwon, W. Kim, S. Park, S. Hong, J. Kim, *Tissue Eng. Regener. Med.* **2021**, 19.
[40] Z. S. Patel, M. Yamamoto, H. Ueda, Y. Tabata, A. G. Mikos, *Acta Biomater.* **2008**, *4*, 1126.
[41] N. Sahoo, R. K. Sahoo, N. Biswas, A. Guha, K. Kuotsu, *Int. J. Biol. Macromol.* **2015**, *81*, 317.
[42] C. Coester, K. Langer, H. Von Briesen, J. Kreuter, *J. Microencapsulation* **2000**, *17*, 187.
[43] K. Geh, *Imu* **2018**.
[44] P. Solanki, P. Kaintura, K. Singh, *J. Nanomed. Res* **2015**, *2*, 00018.
[45] E. IAWA Journal, *IAWA Journal 13*, 455.
[46] A. Avellan, J. Yun, Y. Zhang, E. Spielman-Sun, J. M. Unrine, J. Thieme, J. Li, E. Lombi, G. Bland, G. V. Lowry, *ACS Nano* **2019**, *13*, 5291.
[47] G. Lv, C. Du, F. Ma, Y. Shen, J. Zhou, *ACS Omega* **2018**, *3*, 3548.
[48] E. Manzoor, Z. Majeed, S. Nawazish, W. Akhtar, S. Baig, A. Baig, S. M. Fatima Bukhari, Q. Mahmood, Z. Mir, S. Shaheen, *Agriculture* **2022**, *12*, 1743.
[49] H. T. Wilson, M. Amirkhani, A. G. Taylor, *Front Plant Sci* **2018**, *9*, 1006.
[50] H. Wilson, K. Xu, A. Taylor, *Sci. World J.* **2015**, *2015*.
[51] Z. Zhu, X. Xu, B. Cao, C. Chen, Q. Chen, C. Xiang, G. Chen, J. Lei, *Plant Cell, Tissue and Organ Culture (PCTOC)* **2015**, *120*, 919.
[52] A. Ruggiero, P. Punzo, S. Landi, A. Costa, M. J. Van Oosten, S. Grillo, *Horticulturae* **2017**, *3*, 31.
[53] L. Santuari, G. F. Sanchez-Perez, M. Luijten, B. Rutjens, I. Terpstra, L. Berke, M. Gorte, K. Prasad, D. Bao, J. L. Timmermans-Hereijgers, *Plant Cell* **2016**, *28*, 2937.
[54] C. Galinha, H. Hofhuis, M. Luijten, V. Willemsen, I. Blilou, R. Heidstra, B. Scheres, *Nature* **2007**, *449*, 1053.
[55] P. Křeček, P. Skůpa, J. Libus, S. Naramoto, R. Tejos, J. Friml, E. Zažímalová, *Genome Biol.* **2009**, *10*, 249.
[56] Y. Tao, J.-L. Ferrer, K. Ljung, F. Pojer, F. Hong, J. A. Long, L. Li, J. E. Moreno, M. E. Bowman, L. J. Ivans, *Cell* **2008**, *133*, 164.
[57] J. Kleine-Vehn, J. Friml, *Annu. Rev. Cell Dev. Biol.* **2008**, *24*, 447.
[58] H.-Z. Wang, K.-Z. Yang, J.-J. Zou, L.-L. Zhu, Z. D. Xie, M. T. Morita, M. Tasaka, J. Friml, E. Grotewold, T. Beeckman, *Nat. Commun.* **2015**, *6*, 8822.
[59] J. Jeon, C. Cho, M. R. Lee, N. Van Binh, J. Kim, *Plant Cell* **2016**, *28*, 1828.
[60] Y. Hu, M. Omary, Y. Hu, O. Doron, L. Hoermayer, Q. Chen, O. Megides, O. Chekli, Z. Ding, J. Friml, *Nat. Commun.* **2021**, *12*, 1657.
[61] Q. Tian, J. W. Reed, *Development* **1999**, *126*, 711.
[62] R. C. Burkart, V. I. Strotmann, G. K. Kirschner, A. Akinci, L. Czempik, A. Dolata, A. Maizel, S. Weidtkamp-Peters, Y. Stahl, *EMBO Rep.* **2022**, *23*, e54105.
[63] W. Ramakrishna, R. Yadav, K. Li, *Applied Soil Ecology* **2019**, *138*, 10.
[64] K. Vishwakarma, N. Kumar, C. Shandilya, S. Mohapatra, S. Bhayana, A. Varma, *Front Microbiol* **2020**, *11*, 560406.
[65] R. D. Wauchope, W. C. Johnson, H. R. Sumner, *J. Agric. Food Chem.* **2004**, *52*, 7056.
[66] Z. P. ZHANG, *Weed Biol. Manage.* **2003**, *3*, 197.
[67] R. J. Gilliom, J. E. Barbash, C. G. Crawford, P. A. Hamilton, J. D. Martin, N. Nakagaki, L. H. Nowell, J. C. Scott, P. E. Stackelberg, G. P. Thelin, D. M. Wolock, *Pesticides in the Nation's Streams and Ground Water*, Reston, VA, **2006**, *1992*, 1291.
[68] Y. M. Lvov, D. G. Shchukin, H. Möhwald, R. R. Price, *ACS Nano* **2008**, *2*, 814.
[69] Q. Yu, S. Powles, *Plant Physiol.* **2014**, *166*, 1106.
[70] F. Torralbo, D. Boardman, J. H. Houx III, F. B. Fritschi, *Plant Soil* **2022**, *475*, 551.
[71] J. Tang, J. Hong, Y. Liu, B. Wang, Q. Hua, L. Liu, D. Ying, *J. Polym. Environ.* **2018**, *26*, 1930.
[72] P. Zhang, R. Zhang, X. Fang, T. Song, X. Cai, H. Liu, S. Du, *J. Hazard. Mater.* **2016**, *317*, 543.
[73] H. Hagendorfer, C. Lorenz, R. Kaegi, B. Sinnet, R. Gehrig, N. V. Goetz, M. Scheringer, C. Ludwig, A. Ulrich, *J. Nanopart. Res.* **2010**, *12*, 2481.
[74] N. Ha, E. Seo, S. Kim, S. J. Lee, *Sci. Rep.* **2021**, *11*, 11556.
[75] T. Buie, J. McCune, E. Cosgriff-Hernandez, *Trends Biotechnol.* **2020**, *38*, 546.
[76] R. Sowmya, V. G. Warke, G. B. Mahajan, U. S. Annapure, *Ind Crops Prod* **2023**, *197*, 116577.
[77] M. M. Pour, R. Saberi-Riseh, R. Mohammadinejad, A. Hosseini, *Int. J. Biol. Macromol.* **2019**, *133*, 603.
[78] H. Jing, L. C. Strader, *Int. J. Mol. Sci.* **2019**, *20*, 486.
[79] R. Jacoby, M. Peukert, A. Succurro, A. Koprivova, S. Kopriva, *Front Plant Sci* **2017**, *8*, 1617.
[80] C. Yeguerman, E. Jesser, M. Massiris, C. Delrieux, A. P. Murray, J. O. Werdin González, *Ecotoxicol. Environ. Saf.* **2020**, *189*, 110047.
[81] A. R. Panizzi, J. R. Parra, *Insect bioecology and nutrition for integrated pest management*, CRC press, New York, USA **2012**.
[82] M. Yu, J. Yao, J. i. Liang, Z. Zeng, B. o. Cui, X. Zhao, C. Sun, Y. Wang, G. Liu, H. Cui, *RSC Adv.* **2017**, *7*, 11271.
[83] Y. Nazarenko, T. W. Han, P. J. Lioy, G. Mainelis, *Journal of Exposure Science & Environmental Epidemiology* **2011**, *21*, 515.
[84] J. Park, Y. O. Ahn, J.-W. Nam, M.-K. Hong, N. Song, T. Kim, G.-H. Yu, S.-K. Sung, *Pestic. Biochem. Physiol.* **2018**, *152*, 38.